Oxide characterization of copper cold spray feedstock powders with X-ray photoelectron spectroscopy

Katsari, Christina Maria; Kotsakis, Yannis; Yue, Stephen; Guerreiro, Bruno; Poirier, Dominique; Giallonardo, Jason D.

Publisher's version / Version de l'éditeur:
https://doi.org/10.31399/asm.cp.itsc2023p0091
Thermal Spray 2023: Proceedings from the International Thermal Spray Conference, International Thermal Spray Conference, pp. 91-97, 2023-05-22

Oxide characterization of copper cold spray feedstock powders with X-Ray Photoelectron Spectroscopy

Christina Maria Katsari, Yannis Kotsakis, Stephen Yue
Materials Engineering Department, McGill University, Montreal, Quebec, Canada
christina.katsari@mail.mcgill.ca, ioannis.kotsakis@mail.mcgill.ca

Bruno Guerreiro, Dominique Poirier
National Research Council of Canada(NRC), Boucherville, Quebec, Canada

Jason D. Giallonardo
Nuclear Waste Management Organization (NWMO), Toronto, Ontario, Canada

Abstract

In conventional powder processing, there has been considerable work on classifying feedstock powders based on particle size distribution, morphology, microstructure and composition, since these influence processability and final properties. Cold spray is a new application for powders and conventional characterization may be insufficient to assess powder cold sprayability. In particular, metallic powders have an oxide layer, which breaks during impact with the substrate or with another coating layer during cold spray; this fragmentation facilitates bonding. It has been suggested that the thickness of the oxide layer can influence the mechanism of fragmentation; thicker oxides are easier to remove, revealing clean metal surfaces that can metallurgically bond. Consequently, not all high-purity powders or powders that are stored in ambient conditions have the potential to give good coating properties after cold-spray. This work focuses on surface oxidation of the powders, characterizing the variation of oxide film aspects with size and composition of nominally pure copper powders using X-ray Photoelectron Spectroscopy (XPS). The results indicate the presence of Cu (I) and Cu (II) oxide species on the surface of as-received, naturally aged and heat-treated powders; their thickness is determined using the depth profiling feature.

Introduction

Copper (Cu) powders have been used as feedstock material in the cold-spray process to create coatings that can be used where corrosion protection [1-2] and high electrical conductivity [2] are needed. It has been reported by many researchers that the characteristics of the powder are affecting the final properties of the coating [1-5]. These include, but are not limited to, morphology, chemical composition, particle size distribution and hardness. Since cold spray is a relatively new processing technology for powders, it is still unclear how each individual characteristic, or their cumulative effect, is affecting the final properties of the coating. As an example, it has been reported that the oxygen content, and therefore the amount of oxide present on the powder particles can influence the bonding [6-12]. Specifically, it is generally accepted [6-11] that the more oxygen in the powder, the worse is the metallurgical bonding, the rationale being that the oxygen is present as an oxide, which inhibits metal to metal contact. In contrast, Luo et al. [12] hypothesizes that the thicker the oxide, the easier it is to fragment and peel-off, revealing clean metal surfaces that can metallurgically bond. In addition, previous work [13] on Cu powders suggested that there is a need to properly characterize the powders before spraying, as there was variability in the final properties even from powders from the same specification. In this work, an attempt to use characterization techniques, such as X-Ray Photoelectron Spectroscopy, to characterize the surface oxides and therefore identify potential differences among powders that are otherwise similar (e.g., same chemical composition) is attempted, with the ultimate goal of having a screening tool for the feedstock before cold-spraying.

Experimental methods

Two copper powders, produced by gas atomization at 5N Plus, were selected to study the effect of particle size distribution (fine and coarse). The powders came from the same lot, and the size differences were generated by sieving. A different lot from 5N Plus (HighImp) was selected due to high impurity levels (i.e., Si,Al,Fe) to evaluate the difference, if any, between compositions. The chemical composition was determined by Inductively Coupled Plasma Spectroscopy (ICP) from the manufacturer for all elements except oxygen, which was measured by Instrumental Gas Analysis (IGA). Chemical composition for the powders are presented in Table 1. The elements which are potentially present but are below the detection limit of the instrument, are shown with the "less than" symbol in the Table, where the number represents the detection limit value.

Table 1: Powder chemical composition in ppm by weight

	Fine	Coarse	HighImp
Al	1.4	1.4	688
Fe	3.6	3.6	43
Ni	<2	<2	<2
Zn	<2	<2	<2
As	<5	<5	<5
Ag	<1	<1	14
Cd	0.3	<0.2	<0.2
In	<10	<10	<10
O	88	69	111
Se	<5	<5	<5

Sn	6.3	<5	7
Sb	<5	<5	<5
Au	<0.5	<0.5	<0.5
Pb	<10	<10	<10
Bi	<20	<20	<20
Si	6.5	9.2	1550
S	<20	<20	-
Mn	0.3	0.3	2

The powders were tested in 3 conditions: as-received, naturally aged and heat treated. All powders in the as-received (AR) condition were stored in a desiccator to minimize oxidation upon reception. The naturally aged (NA) powders were kept in ambient atmosphere for 5 days. The heat treatments were performed in an infrared furnace (E4 ChamberIR Heater from Research Inc.), where a quartz tube provided argon gas flow (4 L/min). The apparatus used to hold the alumina crucibles (25mm height X 25mm diameter) in the furnace can be seen in Fig. 1. A stainless-steel mesh filtered the gas flow, while a hole in the middle allowed for contact of the K-type thermocouple that was connected to the temperature controller and in contact with the sample. The heating rate was 1ºC/s until it reached 150ºC. After a consistent soaking time of 10 minutes on all samples the aging time was set to 5 and 60 minutes. These conditions are called HT-5 and HT-60 respectively. Following this, the powders were furnace cooled to ambient temperature (i.e., < 40 ºC) with the argon gas flow on until their removal from the furnace.

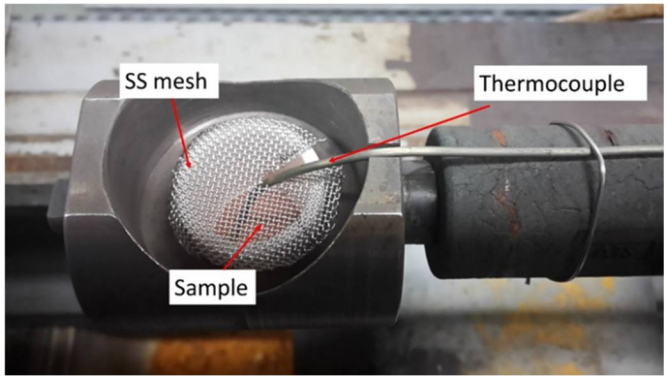

Figure 1: Heat treatment apparatus

Microtrac Flow Sync wet laser diffraction (S/N: HF0114) system was used to measure the particle size distribution (PSD) of all four powders. The powders were dissolved in deionized water and sonication was conducted for two minutes before the analysis.

For microstructural observation, a Hitachi 3500 Scanning Electron Microscope (SEM, S/N 351316-05) coupled with Electron Dispersive Spectroscopy (EDS) was used for high magnification imaging as well as compositional verification. The powders were put directly on a carbon tape to observe into the SEM.

A Thermo-Scientific K-Alpha X-Ray Photoelectron Spectrometer was used to characterize the surface oxide of the powders as well as the depth profiling (etching) feature for 30-600 s with sputter rate estimate in Ta_2O_5=0.2nm/sec, to investigate the presence of oxidation below the surface. The sputter rate estimate of 0.2nm/s was achieved by an ion beam of 1000 eV energy and medium current in a 2 mm^2 area. The energy calibration was based on the carbon peak (C-C,C-H) at binding energy value of 284.8eV. Then, the remaining spectra were shifted by x eV, where x was the difference of the measured binding energy value of carbon and the literature value of 284.8eV. The background used for carbon and copper peaks was Shirley. All spectra were calibrated and analyzed with CasaXPS software. The high-resolution spectra were collected in the following order: Cu 2p, Cu LMM Auger peak, C 1s, O 1s and then a Survey spectrum (long range scan) to avoid degradation of Cu (II) to Cu(I) [14] and to confirm that there were no other elements present.

Results and Discussion

In Table 1, the chemical composition of the three powders indicated that even the powders from the same lot have some small compositional difference determined from ICP (i.e., elements such as Si, Cd and Sn) as well as difference in oxygen. The fine powder had the highest value for oxygen. In comparison, the HighImp powder lot had the highest oxygen along with other impurities as high as two and three orders of magnitude, e.g., Al, Fe and Si. To analyze any differences in size, the PSD in the as-received condition of the three powders were measured and the results presented in Table 2:

Table 2: Particle Size Distribution in um

	D_{10}	D_{50}	D_{90}
Fine	22	30	43
Coarse	52	69	95
HighImp	31	43	62

In terms of morphology, all four powders were spherical as shown in their respective SEM images (see Fig.2).

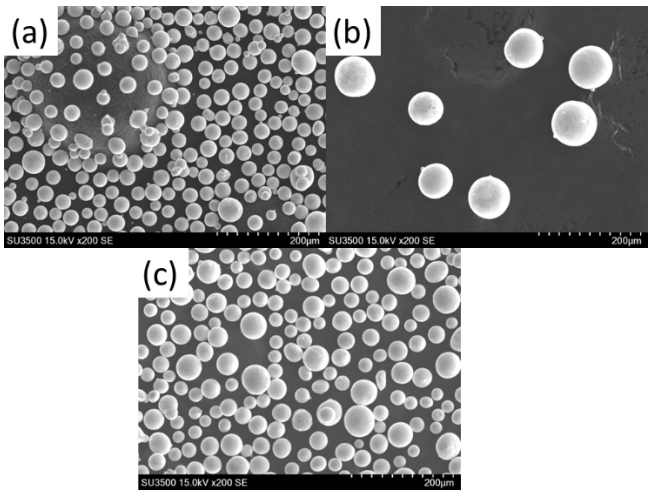

Figure 2: Secondary Electron Images of as received powders. (a)Fine, (b),Coarse and (c)HighImp. Population density of images is related to sampling.

The average specific surface area for the spherical powders can be calculated from the D_{50} by using the formula area/volume or $(4\pi*R^2)/(4/3\pi*R^3) = 3/R$, where R is $D_{50}/2$, and is presented in Table 3:

Table 3: Powder specific surface area (um^{-1})

	D_{50}	Average Specific Surface Area
Fine	30	0.20
Coarse	69	0.09
HighImp	43	0.14

The specific surface areas of fine and coarse (Table 3) indicate that intuitively, the fine should have approximately double the oxygen content if all of it was found as surface oxide layer of same thickness and composition. This is not observed here (see Table 1), indicating that oxide layer characteristics vary with powder sizes.

The powder oxides were characterized by X-Ray Photoelectron Spectroscopy (XPS). The presence of surface oxide is indicated qualitatively by the presence of shake-up satellite peaks in the Cu 2p peak, as well as from the shape of the peak in the Cu LMM Auger peak. Furthermore, with the formulae described in [14], the percentage of Cu (II) and [Cu (I) + Cu (0)] species can be calculated by fitting the corresponding peaks where they contribute, i.e., in the main peak, there are contributions from all three species while in the satellite peak the signal is purely from Cu (II) [14]. The fitting with the Gaussian-Lorentzian values as well as the energy calibration values of the carbon peak were based in [14], aiming a residual as close to 1 as possible. It is worth highlighting that it is not possible to differentiate the metallic species [Cu (0)] from the Cu (I) due to the same binding energy value (933 eV).
The surface Cu 2p scan and Cu LMM scan of all four powders in the as received condition qualitatively indicates the presence of oxide as there is a distinct shake-up peak. An example of the Cu 2p and the Cu LMM scans of the surface can be seen in Figs.3 and 4, respectively.

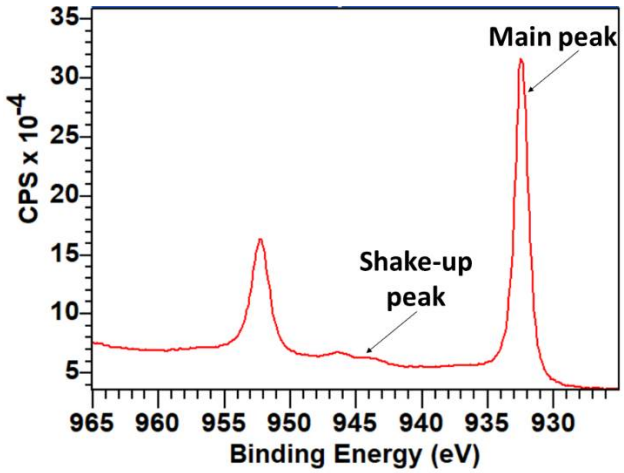

Figure 3: Representative spectrum of Cu 2p scan from the fine powder in the as received condition on the surface

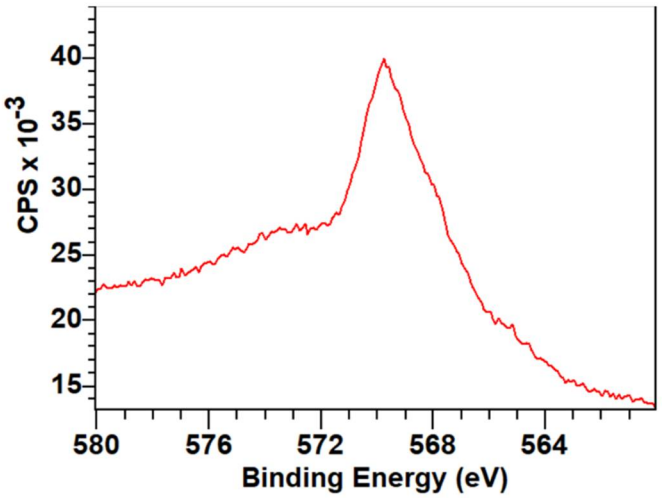

Figure 4: Representative spectrum of Cu LMM scan from the fine powder in the as received condition on the surface

After 30 seconds of etching, which corresponds to 6 nm depth in Ta_2O_5, the Cu 2p satellite peak has visibly less intensity than the surface scan and the Cu LMM starts resembling more the metallic shape, as can be seen in Figs. 5 and 6 respectively.

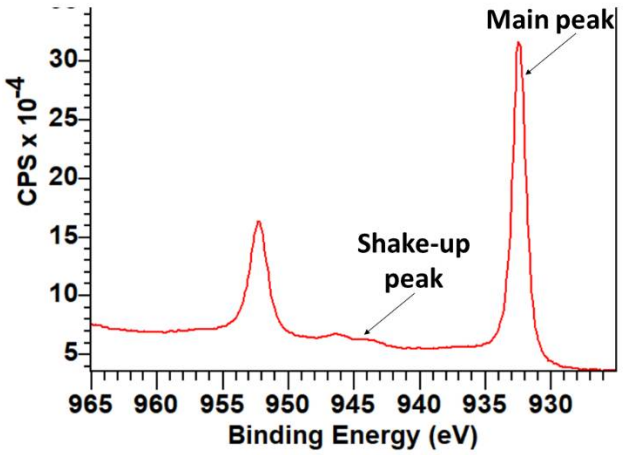

Figure 5: Representative spectrum of Cu 2p scan from the fine powder in the as received condition after 30 seconds of etching

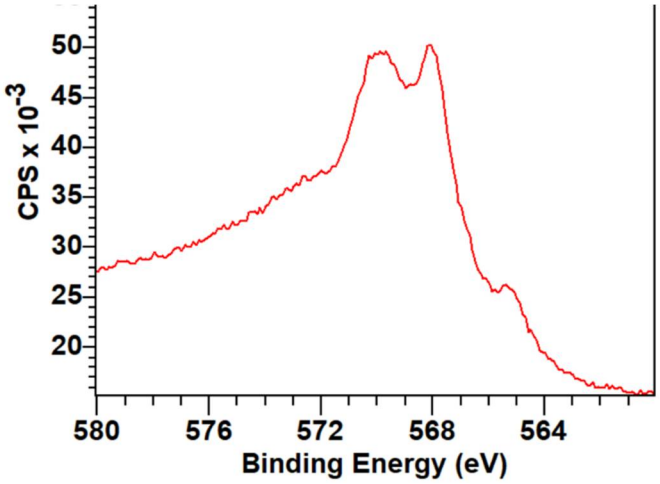

Figure 6: Representative spectrum of Cu LMM scan from the fine powder in the as received condition after 30 seconds of etching

With further etching for 300 seconds (a total of 330 seconds i.e., equivalent depth of 66 nm) and up to 600 seconds (equivalent depth of 120 nm) there is no visible shake-up peak in the Cu 2p scan and the Cu LMM shape is similar to that in the literature of pure metal (i.e., [14]), as can be seen in Fig. 7 and Fig.8 respectively.

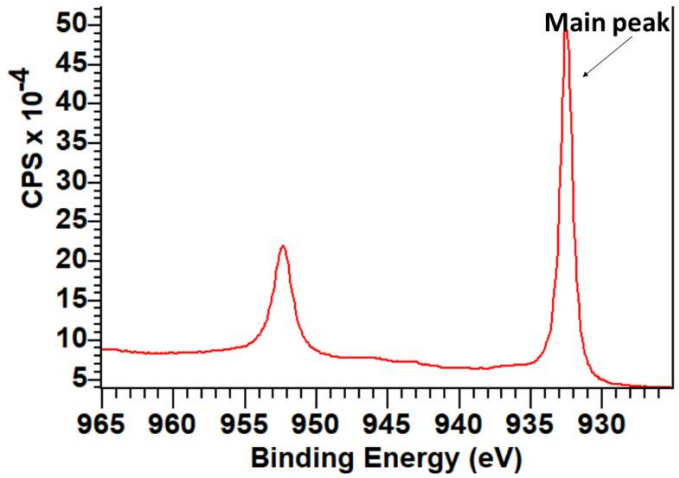

Figure 7: Representative spectrum of Cu 2p scan from the fine powder in the as received condition after 600 seconds of etching

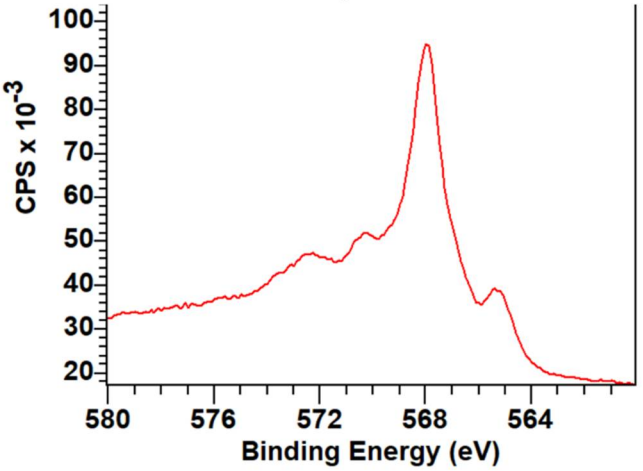

Figure 8: Representative spectrum of Cu LMM scan from the fine powder in the as received condition after 600 seconds of etching

Similarly, for the HighImp powder, after 60 seconds of etching, the Cu 2p scan does not show presence of the shake-up peak (Fig.9).

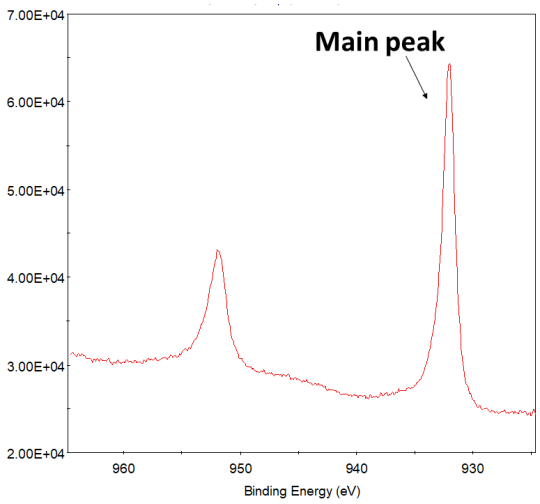

Figure 9: Representative spectrum of Cu 2p scan from the HighImp powder in the as received condition after 60 seconds of etching

Therefore, for the remaining experiments, the focus for oxide characterization included only the first two steps, 0 etching and 30 seconds.

Quantitatively, from the equations derived in [14], the fine powder in the as-received condition has 13±2% Cu (II) on the surface and after 30 seconds of etching it drops to 6±2%. Similarly, but in higher percentage, the coarse powder from 25±7% on the surface, there was 11±2% at 6 nm equivalent depth, i.e. after 30 seconds of etching. The highest Cu (II) percentage was found in the HighImp, with 33±10% on the surface. In terms of existing O, HighImp had the highest percentage (111 ppm), but the fine, which had higher O %, has less Cu (II) on the surface than the coarse. Since HighImp had other elements that could form oxides on the surface, such as Al and Fe and, for the remaining percentage, it is not possible to identify if the % is Cu(I) oxide or Cu (0) metal, it was decided to further investigate the effect of size, i.e., fine versus coarse after natural aging and artificial aging.

In Fig. 10, a strong satellite peak can be observed, which is significantly different qualitatively than the as-received condition. Indeed, after heat treatment at 150°C for 5 and 60 minutes, the Cu (II) oxide percentage increased, but there was no significant difference between the 5 and 60 min (Fig. 11).

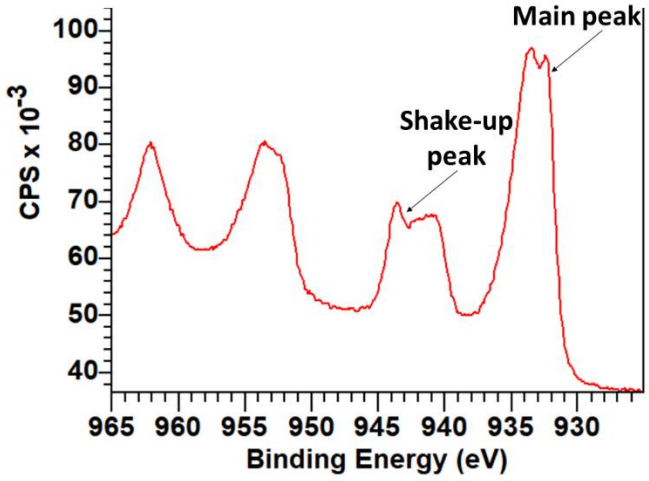

Figure 10: Representative spectrum of Cu 2p scan from the fine powder heat treated at 150°C for 60 minutes, no etching

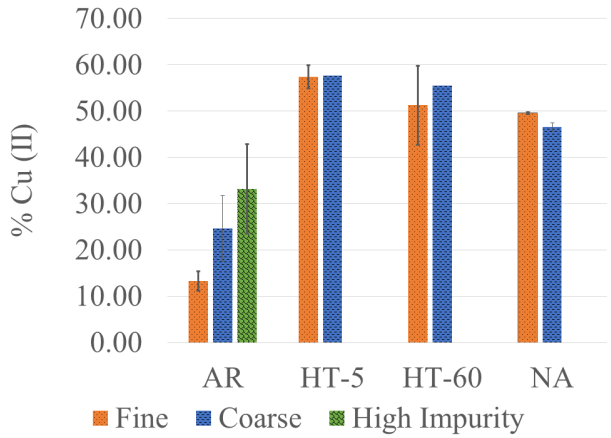

Figure 11: %Cu (II) in as-received, heat treated for 5 minutes heat treated for 60 minutes and natural aging for 5 days surface (no etching)

After natural aging for 5 days, the fine powder consists of 50 ±0.2% Cu (II) on the surface and after 30 seconds of etching it drops to 15±2%. This value is similar to the surface scan in the heat-treated for 60 minutes condition. The shape of the Cu 2p scan is presented in Fig.12.

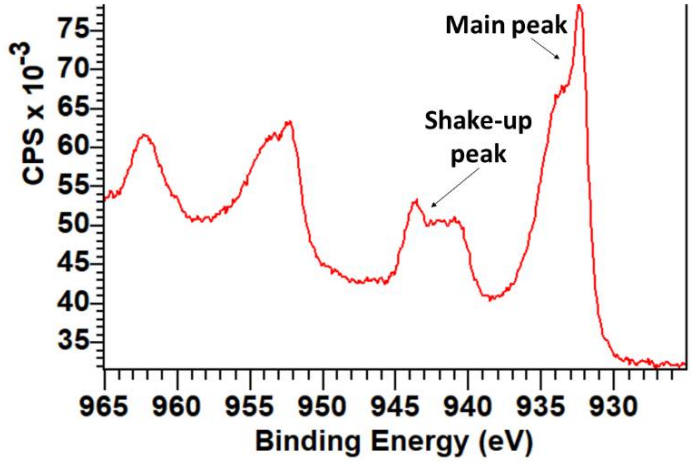

Figure 12: Representative spectrum of Cu 2p scan from the fine powder in the natural aging condition on the surface (no etching)

The coarse powder, after 5 days of natural aging shows 47±1% on the surface and 12±1% after 30 seconds of etching. These percentages are similar to the heat treated coarse powder and also they do not differ much from the natural aged fine powder, which is the same trend with the heat treated conditions.

The heat treatment and natural aging were chosen as an indirect method of comparing "similar" powders. The temperature of 150°C was selected by taking into consideration thermodynamic calculations using FactSage software, where it showed that there was no precipitation below 750°C, only oxides were present. Furthermore, the chosen temperature was below the residual stress temperatures (200-350°C) that have been used in bulk strip forms [15], and the maximum time was the same. In [16], Castrejón-Sánchez et al mention that

temperatures lower than 200 °C showed mainly a thin layer of surface cuprous oxide [Cu(I)], which could not be observed in this work either in the 5 min nor in the 60 min hold for both fine and coarse powder solely from the XPS results. In fact, in [16] a heat treatment of 24 h in protective gas at 1000°C or for 8 h in oxygen formed pure and high crystallinity Cu (II) oxide. This agrees with [17], where the initial oxidation started at 150 °C, but a crystalline phase of the Cu(I) oxide was observed only above 200 °C, and the Cu(II) only above 320 °C, which again does not agree with this work. The difference with [16] and [17] and this work can be attributed to the fact that Cu was in sheet [16] and thin film [17] form, whereas powders have higher surface to volume ratio, therefore the oxidation reaction that could be achieved at lower temperatures, even as low as room temperature (natural aging condition).

It seems that both heat treatment and natural aging did not show any variance between powders with different size. Nevertheless, in the as-received condition, there is a significant difference among them, which does not follow the chemical composition, i.e., the fine has more oxygen but less Cu (II) oxide. This could be attributed to powder manufacturing environment, since although they came from the same lot, there is a different cooling rate in order to create the particle size distribution with fine having a much faster cooling rate than the coarse, since it has about half its average size [18].

It is also worth noting that with XPS, there is a limitation in the characterization of the Cu(I) oxide due to the same binding energy of the metallic Cu, which could explain the inverse trend of the composition with the oxidation, i.e., the remaining oxygen could be in Cu(I) oxide form.

Conclusions and future work

Four Cu powders were analyzed using X-Ray Photoelectron Spectroscopy to identify variations in surface composition among them. It was found that powders from the same lot but different sizes had a significant difference in the presence of Cu (II) oxide in the as-received condition but did not show a distinct difference after heat treatment and natural aging. This could be attributed to manufacturing conditions as well as lack of Cu(I) identification by XPS. The next steps include additional powder characterization with TEM diffraction, to confirm presence of one oxide and metal [i.e., Cu (II) and Cu (0)] or two oxides and metal [i.e., Cu(II),Cu(I) and Cu(0)] .

Acknowledgments

The authors would like to acknowledge the financial support from the Natural Sciences and Engineering Research Council of Canada (NSERC) and Le Consortium de recherche et d'innovation en transformation métallique (CRITM). Also, the powder supplied by 5N Plus is greatly appreciated.

References

1. D. Poirier et al., "*Powder Development and Qualification for High-Performance Cold Spray Copper Coatings on Steel Substrates*", J Therm Spray Tech (2019) 28:, 444–459
2. Koivuluoto, H., Coleman, A., Murray, K. *et al.* High Pressure Cold Sprayed (HPCS) and Low Pressure Cold Sprayed (LPCS) Coatings Prepared from OFHC Cu Feedstock: Overview from Powder Characteristics to Coating Properties. *J Therm Spray Tech* **21**, 1065–1075 (2012). https://doi.org/10.1007/s11666-012-9790-x
3. Guerreiro, B., Vo, P., Poirier, D. *et al.* Factors Affecting the Ductility of Cold-Sprayed Copper Coatings. *J Therm Spray Tech* **29**, 630–641 (2020). https://doi.org/10.1007/s11666-020-00993-z
4. Munagala, V.N.V., Akinyi, V., Vo, P. *et al.* Influence of Powder Morphology and Microstructure on the Cold Spray and Mechanical Properties of Ti6Al4V Coatings. *J Therm Spray Tech* **27**, 827–842 (2018). https://doi.org/10.1007/s11666-018-0729-8
5. Assadi, H., Kreye, H., Gärtner, F., & Klassen, T. J. A. M. Cold spraying–A materials perspective. *Acta Materialia*, **116**, 382-407(2016).
6. Ross, K. A., Lareau, J. P., Glass, S. W., & Meyer, R. M. (2021). *Assessment of Cold Spray Technology for Nuclear Power Applications* (No. PNNL-30299). Pacific Northwest National Lab. (PNNL), Richland, WA (United States).
7. F. Gärtner, T. Stoltenhoff, J. Voyer, H. Kreye, S. Riekehr, M. Koçak, Mechanical properties of cold-sprayed and thermally sprayed copper coatings, Surface and Coatings Technology, Volume 200, Issue 24,2006,6770-6782, https://doi.org/10.1016/j.surfcoat.2005.10.007.
8. Li, Wen-Ya, et al. "Numerical simulation of deformation behavior of Al particles impacting on Al substrate and effect of surface oxide films on interfacial bonding in cold spraying." *Applied Surface Science* 253.11 (2007): 5084-5091.
9. Grujicic, Mica, et al. "Adiabatic shear instability based mechanism for particles/substrate bonding in the cold-gas dynamic-spray process." *Materials & design* 25.8 (2004): 681-688.
10. Kang, Kicheol, et al. "Oxidation dependency of critical velocity for aluminum feedstock deposition in kinetic spraying process." *Materials Science and Engineering: A* 486.1-2 (2008): 300-307
11. Razavipour, Maryam, et al. "Bonding mechanisms in cold spray: Influence of surface oxidation during powder storage." *Journal of Thermal Spray Technology* 30.1 (2021): 304-323.
12. Luo, Xiao-Tao, et al. "Dynamic evolution of oxide scale on the surfaces of feed stock particles from cracking and segmenting to peel-off while cold spraying copper powder having a high oxygen content." *Journal of Materials Science & Technology* 67 (2021): 105-115.
13. Poirier D., Legoux J.G, Vo P., Giallonardo J., Keech P. Powder Development and Qualification for Nuclear Waster Canister Application, North American Cold Spray Conference 2016

14. Biesinger, Mark C. "Advanced analysis of copper X-ray photoelectron spectra." *Surface and Interface Analysis* 49.13 (2017): 1325-1334.
15. Olin Brass Understanding copper alloys: The manufacture and use of copper and copper alloy sheet and strip; Mendenhall, J.H., Ed.; 1977;
16. Castrejón-Sánchez, Víctor-Hugo, et al. "Thermal oxidation of copper over a broad temperature range: towards the formation of cupric oxide (CuO)." *Materials Research Express* 6.7 (2019): 075909.
17. Choudhary, Sumita, et al. "Oxidation mechanism of thin Cu films: A gateway towards the formation of single oxide phase." *AIP Advances* 8.5 (2018): 055114.
18. Gianoglio, D., Ciftci, N., Armstrong, S. *et al.* On the Cooling Rate-Microstructure Relationship in Molten Metal Gas Atomization. *Metall Mater Trans A* **52**, 3750–3758 (2021). https://doi.org/10.1007/s11661-021-06325-2